Physical Properties of Tb^{3+} and Ho^{3+} Ions Embedded in Nanocomposites Phospho-Silicate

E.H. Ahmed[a], A. Amin[a], M.M.H. Ayoub[a], A.I. Hashem[b], and I.K. Battisha[c,*]
[a]Polymers and Pigments Department, National Research Centre (NRC),
33 El Bohouth Str., Dokki, Giza, Egypt
[b]Chemistry Department, Ain Shams University, Cairo, Egypt
[c]Solid State Physics Department, Physics Research Division, National Research Centre (NRC),
33 El Behooth Str., Dokki, Giza, Egypt

(Received July 13, 2019; in final form March 6, 2020)

The use of sol-gel technique to fabricate phospho-silicate nanocomposite SiO_2–P_2O_5 based glasses containing 20 mol.% P_2O_5 deposited on quartz silica substrate is presented in this work. Particularly, terbium Tb^{3+} and holmium Ho^{3+} ions were doped in the mentioned host matrix. A variety of material studies were carried out for the investigation of the physical properties of these new materials, such as the Fourier transform infrared and X-ray diffraction. The X-ray diffraction confirmed that the silica gel crystallization was enhanced as a result of the phosphorus existence. Moreover, the functional groups of the prepared nanocomposite samples were detected from the Fourier transform infrared analyses. The morphology of prepared monolith samples was characterized by high resolution transmission electron microscopy. The surface morphology of both the thin film and monolith samples were confirmed using field emission scanning electron microscopy.

DOI: 10.12693/APhysPolA.137.1037
PACS/topics: nanocomposite, thin film, phospho-silicate and monolith

1. Introduction

Phosphate P_2O_5 is an extremely useful co-dopant for silica as it improves the ability of dissolving the rare-earth ions and provides desirable spectroscopic properties for Tb^{3+} and Ho^{3+} ions [1–4]. In fact, the pure silica is an anomalous host for rare-earth ions which is considered to be an oxide adsorbent [5, 6]. Important spectroscopic parameters of rare-earth ions radiated processes embedded in the oxide nanostructure materials are known as the Judd–Ofelt parameters [7]. It has an important influence on the solid state laser's performance which is governed by the relevant optical characteristics of the active ion and electronic, such as spectral shapes of the emission, cross-section and absorption bands, ion–ion interactions, excited state lifetimes, as well as the static and dynamic ion–lattice interactions. In fact, the presence of silanol groups affect the amorphous silica surface properties, which can act as an oxide adsorbed due to its presence. These groups cause that surface to be hydrophilic at a sufficient concentration.

Integrated optics applications have been used over the past decade. Primary optical integrated circuits (OICs) have been utilized in optical communication, imaging, signal processing, computing, instrumentation, and sensing [7]. The rare-earth ion doped oxide materials have generated a lot of interest, due to their valuable industrial applications in optical potential devices such as sensors, lasers, satellites, telecommunication, display devices, and photonics in the near infrared and visible spectral region. Moreover, the rare-earth impurities are of increasing interest, due to their uniqueness of electrical and optical properties in semiconductor oxide hosts [6, 7]. Their spectroscopic features are affected by the local structure at their sites [6]. The local structure of the rare-earth ions is an important factor such as the arrangement and the type of the legend around the rare-earth ions. Due to these facts we doped the Tb^{3+} and Ho^{3+} ions in phospho-silicate host material for the first time trying to optimize our prepared nanocomposite to be applied as photonic devices application. Their structural properties were evaluated using X-ray diffraction (XRD) and the Fourier transform infrared (FTIR) method, while their morphology were characterized using both field emission scanning electron microscopy (FESEM) and high resolution transmission electron microscopy (HRTEM).

2. Experimental

Nanocomposites phospho-silicates containing 20 mol.% phosphate (SiO_2–20 mol.% P_2O_5) using the tri-ethyl-phosphate as precursor material, symbolic as SP20, were prepared in two different forms: thin film and monolith. First, for the host material silica gel preparation using tetra-ethoxy-silane (TEOS), ethanol (CH_3CH_2OH), distilled water (H_2O) and hydrochloric acid (HCl) as precursor materials. The comprised respective molar ratios were 0.028: 0.174: 0.28: 0.0823 for TEOS: CH_3CH_2OH: H_2O: HCl. Table I summarizes the dopant concentrations, sample abbreviations and the equivalent oxide (mol.%) of the starting precursor materials.

*corresponding author; e-mail: ibattisha@gmail.com

The sol precursor was obtained by mixing (TEOS), ethanol (EtOH, 99.999%, Sigma-Aldrich), and deionized water, with hydrochloric acid acting as catalyst. The prepared nanocomposite systems were obtained in two different forms, namely monolithic and thin film. The prepared samples were obtained by hydrolysis and poly-condensation of tetra-ethoxysilane $(CH_3CH_2OH)_4Si$ (TEOS, 99.999%, Sigma-Aldrich) as SiO_2 precursor, and triethyl-phosphate $(C_2H_5O)_3P(O)$ as P_2O_5 (TEP, 99.999%, Sigma-Aldrich) precursor in ethanol. The sol was hydrolyzed and kept under vigorous stirring at room temperature. Then the holmium Ho^{3+} and terbium Tb^{3+} ions were incorporated in the process, by dissolving $Ho(NO_3)_3$-H_2O (purity 99.9%, Sigma-Aldrich) and $Tb(NO_3)_3$-H_2O (purity 99.9%, Sigma-Aldrich) solutions into the preceding mixture precursors with molar ratios 1 mol.% of Ho^{3+} and Tb^{3+}, respectively, symbolic as follows (SP 1% Ho^{3+}) [SP1HoT] and (SP 1 mol% Tb^{3+}) [SP1TbT] for thin film samples and (SP 1% Ho^{3+}) [SP1HoM] and (SP 1 mol % Tb^{3+}) [SP1TbM] for monolithic samples. These solutions were then filtered with 0.22 μm of sterilized filter membrane. The resultant homogeneous solutions of monolithic materials were filled with molds and aged at room temperature for one week before being dried in the oven at about 60 °C for 21 days until no shrinkage appeared. The final products of monolithic samples were transparent, with no cracks, faint rose color for Ho^{3+} ions and faint white color for Tb^{3+}. Densification of gel was obtained by annealing in air for 3 h at temperatures ranging from 500 °C up to 900 °C in a muffle furnace. The substrates used for application of sol-gel thin films were quartz silica substrates and glass substrates. All substrates were cleaned using an ultra-sonic water bath. All the resultant homogeneous solutions of thin films nanocomposites were dropped and dispersed on optically treated quartz silica substrates and allowed to spin at 3500 rev./min for 30 s by using a homemade spin coater. It is worth pointing out that at least two successive coatings were required to obtain suitable effective film thickness.

2.1. Characterization

XRD was performed on the prepared nanocomposite monolith samples in order to characterize their crystalline structure. The crystallinity of these samples was probed by Philips X-ray difractometer using monochromatic Cu K_{α_1} radiation of wavelength $\lambda = 1.5418$ Å operated at 40 kV and 30 mA. The crystallite size G is determined from the Scherrer equation

$$G = \frac{K\lambda}{D}\cos(\theta),$$

where the Scherrer constant is $K = 0.9$, λ is the wavelength, and D is the full width (in radians) of the peak intensity at half maximum (FWHM). The correction to the measured FWHM D_s for a sample peak was made to accommodate systemic instrumental broadening and utilized peak widths D_q measured from a diffraction scan, taken under identical conditions from a strain-free powdered quartz sample with crystallite size ranging between 5 and 10 μm. The corrected sample peak widths were calculated as $D = \sqrt{D_s^2 - D_q^2}$. Microstrain and crystallite size contributions to D were separated using the Win-Fit program, using standard samples for estimation of instrumental broadening.

TABLE I

Dopant concentrations, sample abbreviations and the equivalent oxide [mol.%] of the starting precursor materials, sintered at different temperatures for 3 h.

Formal starting oxide mixture [mol.%]	Sintered temp. [°C]	Symbols
S20P, Ho^{3+} and Tb^{3+} ions monolith samples		
(SiO_2: 20 P_2O_5), S20P	500 and 900	SP
(SiO_2: 20 P_2O_5: (1 mol.%) Ho_2O_3)	60–900	H[1]60M H[1]500M H[1]700M H[1]900M
(SiO_2: 20 P_2O_5: (1 mol.%) Tb_2O_3)	60 °C–900 °C	Tb[1]60M Tb[1]500M Tb[1]700M Tb[1]900M
Ho^{3+} and Tb^{3+} ions thin film samples		
(SiO_2: 20 P_2O_5: (1 mol.%) Ho_2O_3)	60–900	H[1]60TF H[1]500TF H[1]700TF H[1]900TF
(SiO_2: 20 P_2O_5: (1 mol.%) Tb_2O_3)	60–900	T[1]60TF T[1]500TF T[1]700TF T[1]900TF

The HRTEM allows the user to determine the internal structure of materials. HRTEM was performed by using a high resolution JEOL JEM-2100 equipment operating at 120 kV with attached CCD camera.

Film thickness data and the surface morphology of the prepared samples were depicted by using high resolution field emission gun quanta FEG 250 scanning electron microscopy (HRSEM).

Thermal treatment of the monolithic samples were carried out by using diffractometer (type PW 1390), employing Ni-filtered Cu K. A typical sample weight was about 8–10 mg and the analyses were performed at a heating rate of 10 °C/min from 50 °C to 800 °C under nitrogen atmosphere. The FTIR transmittance spectra were recorded on JASCO, FT-IR, 6100, made in Japan by using KBr pellets.

3. Results and discussion

Homogeneous and crack-free prepared thin films were obtained for all the nanocomposite prepared films symbolically referred to H[1]60-900TF and T[1]60-900TF, respectively.

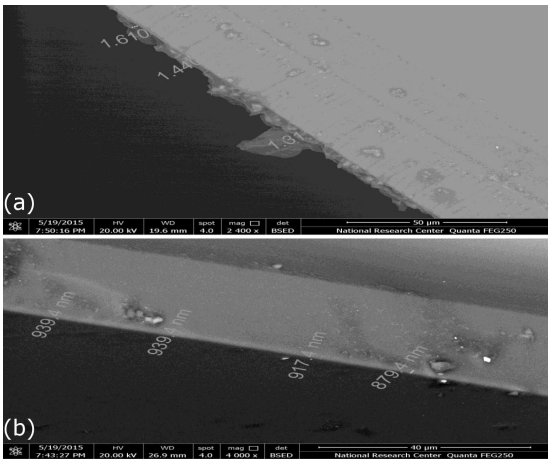

Fig. 1. HRSEM cross section figures of (a) H[1]500TF and (b) T[1]500TF, respectively.

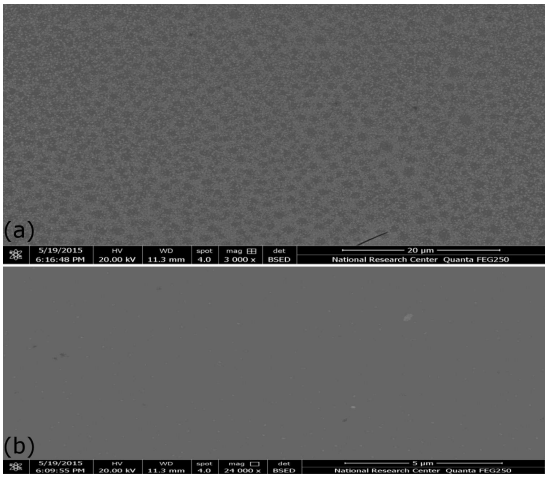

Fig. 2. HRSEM of (a) H[1]500TF and (b) T[1]500TF, respectively.

Figure 1a and b, as representative one, presented the HRSEM cross-section view for H[1]500TF and T[1]500TF, respectively. The thicknesses averages were found to be equal to 1.4536 μm and 918.9 nm for the doped samples with 1 mol.% of both Ho^{3+} and Tb^{3+} ions, respectively.

Figure 2 shows the H[1] 500 TF and T[1]500TF, HRSEM micrographs at two different magnifications 5 and 20 μm. The thin films showed very small sized particles (< 10 nm) and dense SiO_2:P_2O_5 films with homogeneous surface which confirmed the nanostructure phase formation.

The XRD patterns obtained for monolithic samples, i.e., T[1]60M, T[1]900M and H[1]900M, at two different temperatures 60 and 900 °C are shown in Fig. 3a–c, respectively.

For the prepared monolithic samples single diffraction hump at low angle was detected in 2θ range from 18 up to 30° corresponding to amorphous phase, as shown

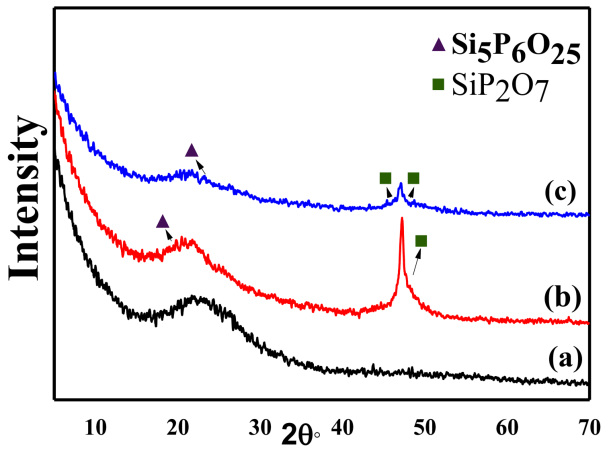

Fig. 3. The XRD diffraction patterns of T[1]60M, T[1]900M and H[1]900M, respectively.

in Fig. 3a. T[1]60M at this lower temperature with similar properties, appeared for H[1]60M, however, due to similarity results were not presented.

The evolution of the XRD patterns as a function of the temperature at 900 °C for the two systems revealed that the crystallization had increased. At higher temperature (900 °C), some phases assigned to (rhombohedra silica phosphate) $Si_5P_6O_{25}$ and (monoclinic silica phosphate) SiP_2O_7 appeared, according to JCPDS cards no. (22-1380), (81-1593), and (71-2073), respectively. In case of $Si_5P_6O_{25}$, it was appeared for both doped samples with Tb^{3+} and Ho^{3+} at $2\theta = 19°$ and 21°, respectively. However, two peaks for monoclinic silica phosphate (SiP_2O_7) appeared at $2\theta = 47°$, according to JCPDS card no. (22-1380) for both kinds of samples with higher intensity for doped sample with Tb^{3+} ions. These results were compatible with the previously reported results by our team work [8], which confirmed that the addition of P_2O_5 into the silicate network led to the enhancement of the crystallization of host materials, where it is well known that the silica gel without the presence of phosphate as dopand at 900 °C is in amorphous phase [8]. Some XRD diffraction features were attributed to the removal of OH and the OR groups from the surface causing an increase in the surface density. By increasing the temperature up to 900 °C a crystalline $Si_5P_6O_{25}$ (rhombohedra silica phosphate) phase appeared as well. This was likely to be due to the sol-gel preparation route, which led to glasses with lower density due to the higher closed porosity than their melt-quenched analogues [9]. The crystal size (i.e. C.S.) values were found to be equal to 20 nm and 23 nm in case of monolith samples H[1]900M and T[1]900M, both sintered at 900 °C. This might be due to the re-crystallization and re-arrangement in the crystalline lattice structure.

The FTIR spectra for all monolith samples dried at 60 °C for 3 weeks, and then sintered at different temperatures 500 °C, 700 °C, and 900 °C for 3 h were measured

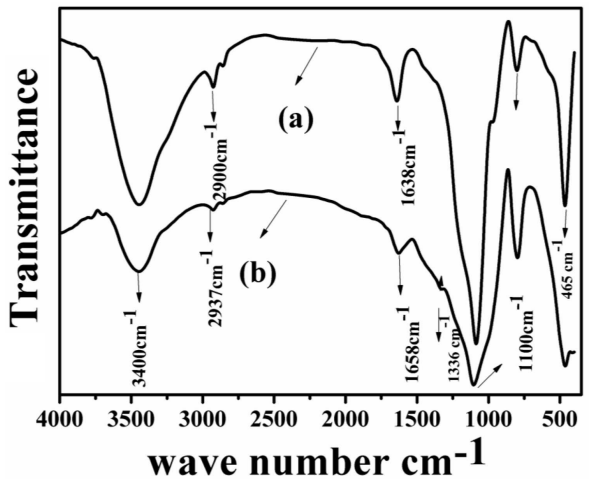

Fig. 4. FTIR spectra of (a) SP and (b) pure SiO_2, respectively, at two different temperature 500 °C and 900 °C.

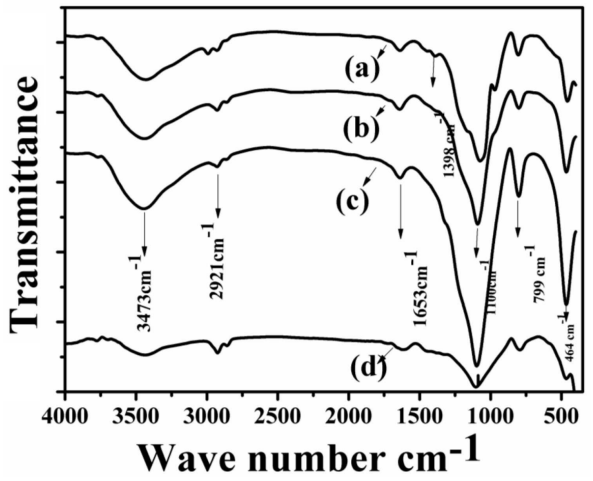

Fig. 5. FTIR spectra of SP1HoM sintered at (a) 60 °C, (b) 500 °C, (c) 700 °C, and (d) 900 °C, respectively.

at (400–4000 cm^{-1}), as shown in Figs. 4–6. The FTIR of the OH stretching peaks for phospho-silicate S20P, sintered at 500 and 900 °C, respectively, is shown in Fig. 4. A wide band appearing at 3400 cm^{-1} was assigned to the OH group. This absorption peaks were attributed to the deformation mode at about 1658 cm^{-1}. The shoulder present at 3695 cm^{-1} was assigned to SiO-H silanol with hydrogen bonding detected.

Figures 5 and 6 indicate the FTIR structural study of the sol-gel glasses with SP doped with two different rare-earth ions Ho^{3+} and Tb^{3+} (marked as SP1HoM and SP1TM) sintered at different temperature 500 °C, 700 °C, and 900 °C for 3 h. At 700 °C, the new small peak at 3777 cm^{-1} appeared due to the free SiO–H silanol. When the samples were heated at 900 °C the OH bands intensity considerably diminished [1]. The Si–O–Si stretching vibration wide band annealed between 1000 and 1250 cm^{-1}, comprised of an intense peak at 109 cm^{-1} and a shoulder around 1220 cm^{-1}. The peak detected

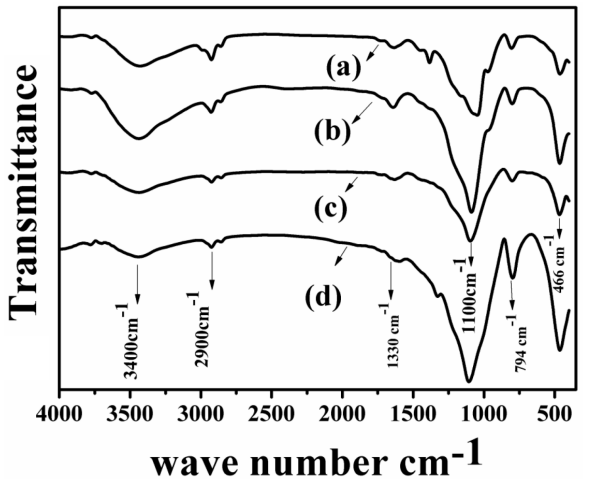

Fig. 6. FTIR spectra of SP1TbM sintered at (a) 60 °C, (b) 500 °C, (c) 700 °C, and (d) 900 °C, respectively.

near 977 cm^{-1} was due to the SiO–H flexion mode. Moreover, the peak appearing near 800 cm^{-1} was due to Si–O vibrations mode and was assigned as characteristic of ring structures inside the glass matrix [11]. The phosphate anions generated a bigger stability, where the sample contained these anions to introduce a higher specific area and higher values of the Lewis sites density. The peak at 1633 cm^{-1} was assigned to H-bonded to water molecular presence and attributed to the deformation mode of adsorbed water molecular in the sample [12]. Presence of these last bands was confirmed by the appearance of another wide band attributed to O–H stretching in the range between 3350 and 3600 cm^{-1}. For P_2O_5 the phosphate groups appeared due to the presence of PO_4^{3-} bending bands. The sol–gel glasses developed important structural details due to the presence of aggregation of clusters during the growth process, where its high porosity allowed the accommodation of water molecules as a result of silanol groups being present in the glass matrix. In fact, the occurrence of this band suggested that the diameters of the pores were bigger than the atomic interstices. This obvious result was in good agreement with the porous character of the sol–gel glasses [11, 12], where phosphor-silicate polycondensation species proceeded quickly during the heating

The constituent particles of nanostructure SP doped with the mentioned two rare-earth elements were depicted from HRTEM, in Fig. 7a for SP1HM and in Fig. 7b for SP1TM, each sintered at different temperatures of 60 °C, 500 °C, and 900 °C, respectively. The particle shapes of all prepared samples were irregular and relatively aggregated molecules with amorphous phase appeared at lower temperature 60 °C. At higher temperature 500 °C and 900 °C, the nanostructure scale was displayed. While the particles became uniform with nearly spherical shape, homogeneous and well-dispersed nanocomposites appeared at these temperatures. In summary, HRTEM revealed high density presence for

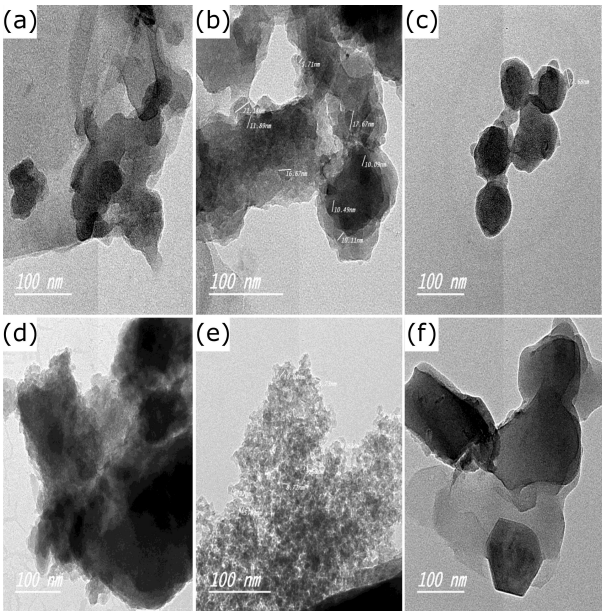

Fig. 7. HRTEM of SP1HoM at (a) 60 °C, (b) 500 °C, and (c) 900 °C, SP1TbM at (d) 60 °C, (e) 500 °C and (f) 900 °C, respectively.

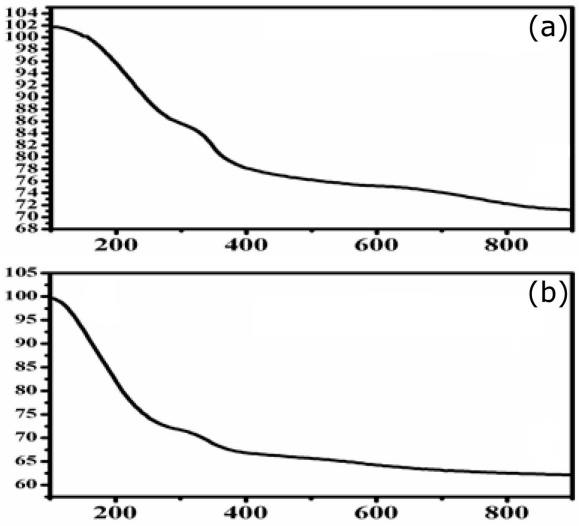

Fig. 8. TGA of (a) SP1HoM and (b) SP1TbM, respectively.

fine volume nucleated crystals in the P_2O_5 containing glasses [11]. It is clear that particles are well dispersed in the preparation process of all prepared samples. Moreover, the nanostructure phase presence was confirmed by obtaining particles with diameters less than 15 nm.

The total weight losses for [SP1HM] and [SP1TM], were 22.3% and 38.08% respectively, as shown in Fig. 8. All samples presented a high thermal stability till 900 °C. The decomposition started for all prepared samples at 110 °C with a weight of 15.2% and 28.8% due to the weakly bound water and loss of alcohols [13, 14]. The recorded weight loss was due to the organic groups' removal and simultaneous removing of water, ethanol, nitrate, and phospho-silicate compounds obtained by sol–gel process [15]. At 800 °C, an increase in the crystalline structure and simultaneous disappearance was detected of the amorphous contribution of the phospho-silicate materials. Additionally, the increase in temperature caused the removal of Si_3 $(PO_4)_4$ phase, while both the (silica phosphate) SiP_2O_7 and (rhombohedra silica phosphate) $Si_5P_6O_{25}$ phases increased. Complete removal of the Si_3 $(PO_4)_4$ phase occurred as a result of phase transformation.

4. Conclusion

Nanocomposites phospho-silicates containing 20 mol% phosphate, (SiO_2–20 mol.% P_2O_5) using the tri-ethyl-phosphate as precursor material (marked as SP20) were prepared in two different forms, thin film and monolith. For the host material silica gel preparation using tetra-ethoxy-silane (TEOS), ethanol (CH_3CH_2OH), distilled water (H_2O), and hydrochloric acid (HCl) as precursor materials, the comprised respective molar ratios were 0.028: 0.174: 0.28: 0.0823 for TEOS: CH_3CH_2OH: H_2O: HCl. The crystallite sizes of the doped samples with 1 mol.% for both Ho^{3+} and Tb^{3+} ions embedded in phospho-silica gel were 20 and 23 nm, respectively, in monolith form sintered at 900 °C. The thicknesses averages were found to be equal to 1.4536 μm and 918.9 nm for the doped samples with 1 mol.% of both Ho^{3+} and Tb^{3+} ions sintered at 500 °C, respectively.

Acknowledgments

This study was funded by Normal Fund of National Research Centre for Ph.D. Student which is 12000 Egyptian pounds.

References

[1] I.K. Battisha, A. Amin, M.M.H. Ayoub, A.I. Hashem, E.H. Ahmed, *Acta Phys. Pol. A* **132**, 1277 (2017).

[2] A. Amin, E.H. Ahmed, M.W. Sabaa, M.M.H. Ayoub, I.K. Battisha, *Polym. Bull. J.* **73**, 147 (2016).

[3] A. Lukowiak, R.J. Wiglusz, A. Chiappini, C. Armellini, I.K. Battisha, G.C. Righini, M. Ferrari, *J. Non-Cryst. Solids* **401**, 32 (2014).

[4] A. Lukowiak, A. Chiappini, A. Chiasera et al., *J. Opt. Quant. Electron.* **47**, 117 (2015).

[5] M.G. Ghanem, Y. Badr, T.A. Hameed, M. El Marssi, A. Lahmar, H.A. Wahab, I.K. Battisha, *Mater. Res. Express* **6**, 085916 (2019).

[6] A. Salah, S.K. El-Mahy, O. El-sayed, I.K. Battisha, *Optik* **209**, 164571 (2020).

[7] C.J. Brinker, G.W. Scherer, *The Physics and Chemistry of Sol-Gel Processing*, Academic, London 1990.

[8] M. Kamal, I.K. Battisha, M.A. Salem, A.M.S. El Nahrawy, *J. Sol-Gel Sci. Technol.* **40**, 507 (2011).

[9] I.K. Battisha, H.H. Afify, I.M. Hamada, *J. Magn. Magn. Mater.* **292**, 440 (2005).

[10] I.K. Battisha, H.H. Afify, M. Ibrahim, *J. Magn. Magn. Mater.* **306**, 211 (2006).

[11] A. Amin, E.H. Ahmed, C. Wickleder, M. Adlung, A.I. Hashem, M.M.H. Ayoub, I.K. Battisha, *Polym. Compos.* **40**, 2029 (2018).

[12] I.K. Battisha, *J. Non-Cryst. Solids* **353**, 1748 (2007).

[13] J.K. Hong, H.S. Yang, H.J. Moon, Y. Choi, *Thin Solid Films* **308-309**, 495 (1997).

[14] P.H. Massiot, M.A. Centeno, M. Gouriou, M.I. Dominguez, J.A. Odriozola, *J. Mater. Chem.* **13**, 67 (2003).

[15] D. Carta, D.M. Pickup, J.C. Knowles, I. Ahmed, E.S. Mark, R.J. Newport, *J. Non-Cryst. Solids* **353**, 1759 (2007).